Proceedings of the 17th World Congress
The International Federation of Automatic Control
Seoul, Korea, July 6-11, 2008

Adaptive Control of Generalised Dynamically Substructured Systems

David P. Stoten* Jia-Ying Tu* Guang Li*

**Advanced Control and Test Laboratory, Department of Mechanical Engineering, University of Bristol (e-mail: D.P.Stoten@bristol.ac.uk, Jiaying.Tu@bristol.ac.uk, Guang.Li@bristol.ac.uk).*

Abstract: The use of the dynamically substructured systems (DSS) approach for engineering testing environments is receiving significant global interest. DSS enables a full-size, critical component to be physically tested within a laboratory environment, whilst the remaining part(s) of the entire system are modelled as a real-time numerical simulation. This paper will present a generalised substructuring framework, using a practical example for illustration. Correspondingly, a linear substructuring control (LSC) strategy is presented, together with a development of the adaptive minimal control synthesis (MCS) algorithm. Comparative simulation results of the two DSS control strategies are also included.

Keywords: Dynamic substructuring, Adaptive control, Minimal control synthesis algorithm, Advanced dynamic testing.

1. INTRODUCTION

Much attention is currently being given to the principle of dynamically substructured systems (DSS) by the worldwide dynamic testing community. The essential principal of DSS is to decompose a complete, or emulated, system ($\sum_E$) into two or more substructures. The substructures must then be synchronised, to behave in exactly the same manner as the emulated system. Often, a critical, possibly nonlinear, substructure is tested physically and the remaining substructure is modelled numerically, both running in real-time. DSS can have the following advantages over more conventional testing schemes (Blakeborough *et al.*, 2001): 1) the critical component is full-size, but physical testing of the entire system is avoided; 2) similitude and nonlinear problems when using scale models are avoided; 3) convergence and stability problems associated with purely numerical simulations are avoided.

(Stoten and Hyde, 2006) presented a first step in the development of a generalised substructuring framework, including the essential control and actuator elements, as shown in Fig.1. Here, a substructured system can be represented by three blocks, $\{G, G_1, G_2\}$, where G_1 is typically related to the numerical substructure ($\sum_N$), G is the interaction constraint associated with both the physical and numerical substructures and G_2 is typically associated with the physical substructure ($\sum_P$). Note that $\{G, G_1, G_2\}$ are not limited to single-input, single-output (SISO) transfer functions. They can also describe multi-input, multi-output (MIMO) systems, in state-space or transfer function matrix forms. Generally, both $\sum_N$ and $\sum_P$ may be comprised of more than one substructure.

In Fig.1, z_1 is the numerical substructure output response to d, the external excitation and z_2 is the measured response from the physical substructure. These outputs must be in near-perfect synchronisation if a DSS is to function satisfactorily, so that in Fig. 1, the substructuring error, e, is always driven to zero by the action of an outer-loop DSS controller.

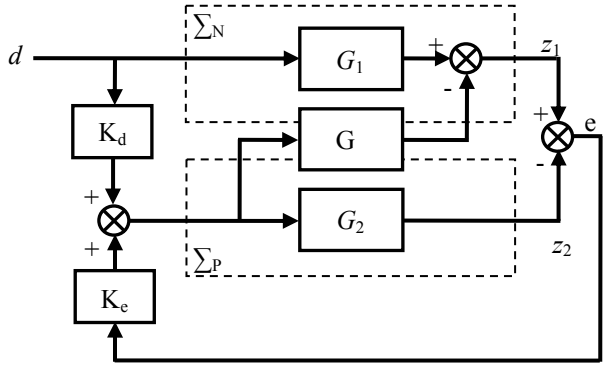

Fig.1. The substructuring framework, with a linear substructuring controller; (Stoten and Hyde, 2006)

A successful DSS controller must be able to cope with unknown, time-varying and nonlinear dynamics in the physical substructure (Bonnet, *et al.*, 2007). The DSS control problem is compounded by the fact that the addition of actuators within $\sum_P$, plus the associated actuator inner-loop controllers, (collectively known as the transfer system), will cause significant synchronisation errors. Therefore, it is vital that a DSS controller must also compensate for such effects.

Thus, the linear substructuring controller (LSC) and the adaptive minimal control synthesis with error feedback (MCSEF) algorithms have both been proposed as viable DSS controllers; (Stoten and Hyde, 2006). As illustrated in Fig.1, LSC is a 2-degree-of-freedom (DOF) controller, where K_e is the feedback loop component and K_d is the forward loop compensator. The gains $\{K_e, K_d\}$ can be synthesised from a complete knowledge of the DSS dynamics. However, it is known that the LSC policy may significantly deteriorate in the presence of nonlinearities and/or unknowns in the dynamics. In such cases the adaptive MCSEF algorithm is

proposed for the control of DSS. The MCSEF controller, which can be used in parallel with LSC, is of the same structure as Fig.1. However, in MCSEF, $\{K_e, K_d\}$ are directly and automatically synthesised as time-varying adaptive gains. The DSS synchronisation error dynamics are then ensured to possess the property of global asymptotic stability.

Hence the principle objectives of this paper are to present a more generalised DSS framework than presented in (Stoten and Hyde, 2006), together with the corresponding LSC and MCSEF control strategies for that framework. In section 2, we will further explore the substructuring technique for more generalised systems than have hitherto been investigated. Section 3 will synthesise the LSC and MCSEF controllers, based upon the developments in section 2. Comparative simulation studies in section 4 will investigate the performance of LSC and MCSEF under some demanding test conditions. Finally, conclusions to the work are drawn together in section 5.

2. A GENERALISED DSS FRAMEWORK

This section investigates a generalised framework for DSS analysis and synthesis. To better illustrate the concepts, we will describe a 2-wheeled, 'quasi-motorcycle' (QM) DSS, currently being developed and built at the University of Bristol. Without loss of generality, this example is used in section 3 to illustrate show how DSS controllers are synthesised. The example is also used in section 4 to show, by way of simulation, the effectiveness of the proposed DSS controllers.

2.1 Substructuring of the QM system

The emulated QM is shown in Fig.2. It is decomposed into three substructures: the front wheel/tyre ($\sum_1$), the rear wheel/tyre ($\sum_2$) and the vehicle rigid body, with front and rear suspension struts ($\sum_3$). The two wheels are excited by external road disturbances, d_1 and d_2. The vehicle body can then have an asymmetric mass distribution, so that the centre of mass is offset from the geometric centre. Relevant parameters are listed in the Appendix, Table 2. In many DSS there is a certain arbitrariness over the selection of the synchronised variables and the interaction constraints. For example, in the QM DSS, the forces ($\{f_{31}, f_1\}$, $\{f_{32}, f_2\}$) and the displacements ($\{y_{31}, y_1\}$, $\{y_{32}, y_2\}$) can either be selected as synchronised variables or interaction constraints.

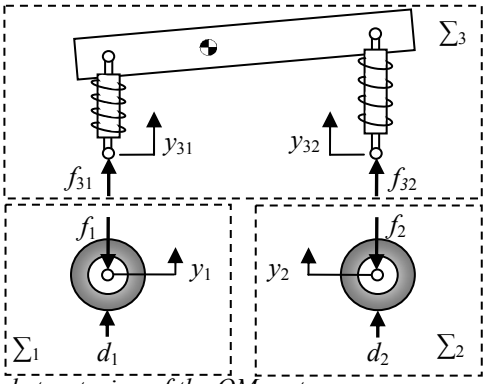

Fig.2. Substructuring of the QM system

In this paper, the original substructuring framework is generalised according to the mode(s) of operation (MO) within the physical substructure(s). In particular, we conceive two main categories of MO: (a) inertial forces are imparted on the test component (*eg.* using a shaking table) and/or (b) reaction forces are imparted onto the test component (*eg.* using a reaction frame). When the DSS contains only one $\sum_P$ with one MO, we say it has a *single-mode* (SiM). Two or more the same type of MO constitute a *multi-mode* (MuM) DSS. If the DSS has different MOs, then it is called a m*ixed-mode* (MiM) system. To complete the set, a DSS which has entirely numerical substructures is said to be a *numerical-mode* (NuM) system and one which has entirely physical substructures is said to be a *physical-mode* (PhM) system.

Table 1 indicates how the five substructuring modes can be applied to the QM system. In the table, N and P denote the numerical and physical substructures, respectively. If either $\sum_1$ or $\sum_2$ is a physical substructure, the imparted forces are of the reaction type, whereas if $\sum_3$ is a physical substructure, the forces are of the inertial type. The table also indicates that the SiM can be categorised as SiM1 or SiM2, since the single MO can either be in $\sum_3$ or in either of $\sum_1$ or $\sum_2$. For example, the QM SiM1 configuration is shown schematically in Fig.3.

Table 1. Substructured MO for the QM

	SiM1	SiM2	MuM	MiM	NuM	PhM
$\sum_1$	N	P	P	P	N	P
$\sum_2$	N	N	P	N	N	P
$\sum_3$	P	N	N	P	N	P

2.2 Synthesis of SiM1 for the QM

At the University of Bristol, we are investigating all of the MO shown in Table 1. However, for the sake of brevity in this paper (and without loss of generalisation), we now concentrate solely on SiM1. From the outset of the SiM1 design, we choose to synchronise displacements and use forces as interaction constraints. The main reason for this choice is that force measurements tend to be relatively noisy, so that displacement control is the preferred option. However, there are situations when force control results in a more well-conditioned controller synthesis procedure. Displacement versus force control issues will be addressed in a subsequent work.

With reference to Fig. 3, the forces, $\{f_{a31}, f_{a32}\}$, are measured by the two actuator load cells and are fed back to the numerical substructures as interaction constraints. Simultaneously, $\{\sum_{N1}, \sum_{N2}\}$ generates two numerical displacement outputs, $\{y_1, y_2\}$, in response to the road disturbances, $\{d_1, d_2\}$, and the above constraint forces. The actuator displacements, $\{y_{a31}, y_{a32}\}$, are controlled via the action of the DSS outer-loop signals, $\{u_{31}, u_{32}\}$. Then, the control objective is to synchronise $\{y_1, y_2\}$ with $\{y_{a31}, y_{a32}\}$ and thereby minimise the substructuring displacement errors, $\{e_{y1}, e_{y2}\}$. Note that Fig. 3 does not explicitly show the inner-loop controls within the actuator systems. These are usually of a basic (PID) nature, supplied as part of a proprietary package, usually having fixed parameters. In this work we

assume that each inner-loop controller/actuator set is combined into one dynamic subsystem.

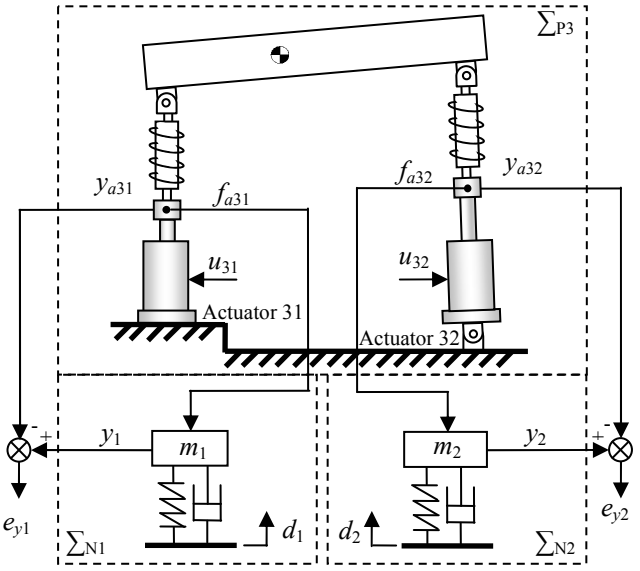

Fig. 3. The first Single-Mode substructured system

Therefore, from Fig. 3, the transformed response of $\sum_{N1}$ is:

$$y_1(s)=\left(\frac{c_1 s+k_1}{m_1 s^2+c_1 s+k_1}\right)d_1(s)-\left(\frac{1}{m_1 s^2+c_1 s+k_1}\right)f_{a31}(s) \quad (1)$$

Where the force f_{a31} is determined from the equations of motion of the rigid body in heave and pitch, together with the corresponding linearised trigonometric relationships in the kinematic equations (*ie* assuming the body angle is small):

$$f_{a31}(s)=\left(\frac{P_2\left(c_{31}s^3+k_{31}s^2\right)}{\frac{L_{32}}{L_3}m_3 s^2+c_{31}s+k_{31}}\right)y_{a31}(s)+\left(\frac{P_3\left(c_{32}s^3+k_{32}s^2\right)}{\frac{L_{31}}{L_3}m_3 s^2+c_{32}s+k_{32}}\right)y_{a32}(s) \quad (2)$$

Note that the linearised relationships are used in section 3 for the synthesis of the LSC controller. However, the full nonlinear dynamics are used in the comparative simulations of section 4.

Similarly, for $\sum_{N2}$:

$$y_2(s)=\left(\frac{c_2 s+k_2}{m_2 s^2+c_2 s+k_2}\right)d_2(s)-\left(\frac{1}{m_2 s^2+c_2 s+k_2}\right)f_{a32}(s) \quad (3)$$

$$f_{a32}(s)=\left(\frac{P_3\left(c_{31}s^3+k_{31}s^2\right)}{\frac{L_{32}}{L_3}m_3 s^2+c_{31}s+k_{31}}\right)y_{a31}(s)+\left(\frac{P_1\left(c_{32}s^3+k_{32}s^2\right)}{\frac{L_{31}}{L_3}m_3 s^2+c_{32}s+k_{32}}\right)y_{a32}(s) \quad (4)$$

where P_1, P_2 and P_3 are equivalent masses associated with the vehicle body dynamics:

$$P_1=\left(\frac{m_3 L_{31}^2}{L_3^2}+\frac{J_3}{L_3^2}\right),\ P_2=\left(\frac{m_3 L_{32}^2}{L_3^2}+\frac{J_3}{L_3^2}\right)$$

$$P_3=\left(\frac{m_3 L_{31} L_{32}}{L_3^2}-\frac{J_3}{L_3^2}\right) \quad (5)$$

A simple first-order transfer function was obtained for each inner-loop controller/actuator set, via a process of system identification:

$$y_{a31}(s)=\left(\frac{b_{31}}{s+a_{31}}\right)u_{31}(s) \quad (6)$$

$$y_{a32}(s)=\left(\frac{b_{32}}{s+a_{32}}\right)u_{32}(s) \quad (7)$$

Substitution of (6) and (7) into (2) and (4) yields the interaction force dynamics in terms of u_{31} and u_{32}. In the following, the interaction forces are then substituted into (1) and (3), generating z_1 (= $[y_1 \ \ y_2]^T$):

$$z_1(s)=\begin{bmatrix}y_1(s)\\ y_2(s)\end{bmatrix}=G_1(s)\underbrace{\begin{bmatrix}d_1(s)\\ d_2(s)\end{bmatrix}}_{d(s)}-G(s)\underbrace{\begin{bmatrix}u_{31}(s)\\ u_{32}(s)\end{bmatrix}}_{u(s)} \quad (8)$$

where G_1 is a 2×2 diagonal transfer function matrix and G is a 2×2 transfer function matrix with interaction dynamics. Similarly, z_2 (= $[y_{a31} \ \ y_{a32}]^T$) is determined from (6) and (7) as:

$$z_2(s)=\begin{bmatrix}y_{a31}(s)\\ y_{a32}(s)\end{bmatrix}=G_2(s)\underbrace{\begin{bmatrix}u_{31}(s)\\ u_{31}(s)\end{bmatrix}}_{u(s)} \quad (9)$$

where G_2 is also a 2×2 diagonal transfer function matrix. Equations (8) and (9) therefore generalise the previous work of (Stoten and Hyde, 2006) into the MIMO domain.

3. SYNTHESIS OF SUBSTRUCTURING CONTROLLERS

3.1 The linear substructuring controller (LSC)

In most of the following we omit the Laplace variable, s, for the sake of brevity. From (8) and (9), the error transfer function, given by $e = z_1 - z_2$, can be written as:

$$\underbrace{\begin{bmatrix}e_{y1}\\ e_{y2}\end{bmatrix}}_{e}=\underbrace{\begin{bmatrix}G_{d11} & 0\\ 0 & G_{d22}\end{bmatrix}}_{G_d}\underbrace{\begin{bmatrix}d_1\\ d_2\end{bmatrix}}_{d}-\underbrace{\begin{bmatrix}G_{u11} & G_{u12}\\ G_{u21} & G_{u22}\end{bmatrix}}_{G_u}\underbrace{\begin{bmatrix}u_{31}\\ u_{32}\end{bmatrix}}_{u} \quad (10)$$

where $G_u = G + G_2$ and $G_1 = G_{d.}$. The MIMO linear substructuring controller, based on the notation of Fig.1, is then proposed as:

$$\underbrace{\begin{bmatrix}u_{31}\\ u_{32}\end{bmatrix}}_{u}=\underbrace{\begin{bmatrix}K_{d11} & K_{d12}\\ K_{d21} & K_{d22}\end{bmatrix}}_{K_d}\underbrace{\begin{bmatrix}d_1\\ d_2\end{bmatrix}}_{d}+\underbrace{\begin{bmatrix}K_{e11} & K_{e12}\\ K_{e21} & K_{e22}\end{bmatrix}}_{K_e}\underbrace{\begin{bmatrix}e_{y1}\\ e_{y2}\end{bmatrix}}_{e} \quad (11)$$

Substituting (11) into (10), the error can be written as:

$$e=\left[I+G_u K_e\right]^{-1}\left[G_d-G_u K_d\right]d \quad (12)$$

We see that (12) implies a 2-DOF control solution, with the first part of the solution, which ensures $e \rightarrow 0$, being given by:

$$K_d = G_u^{-1} G_d \tag{13}$$

assuming that G_u is non-minimum phase and non-singular. Then, closed-loop stability is guaranteed if K_e is determined by selecting the roots of the following decoupled closed-loop characteristic equations in the left-hand s-plane:

$$1 + \left(G_{u11} - \left(\frac{G_{u12} G_{u21}}{G_{u22}} \right) \right) K_{e11} = 0 \tag{14}$$

$$1 + \left(G_{u22} - \left(\frac{G_{u21} G_{u12}}{G_{u11}} \right) \right) K_{e22} = 0 \tag{15}$$

and also assigning the off-diagonal entries of K_e as:

$$K_{e12} = -\left(\frac{G_{u12}}{G_{u11}} \right) K_{e22} \tag{16}$$

$$K_{e21} = -\left(\frac{G_{u21}}{G_{u22}} \right) K_{e11} \tag{17}$$

For example, Fig. 4 respectively shows: (a) the Bode plot for $K_{d11}(j\omega)$, as determined by (13); (b) the roots' loci of the characteristic equation in (14), when K_{e11} is a simple gain; (c) the Bode plot for $K_{e21}(j\omega)$ as determined by (17). In the above roots' loci design, to achieve critical damping of the non-dominant pair at $s = -173 + 0j$, the value of gain is determined as $K_{e11} \approx 35$.

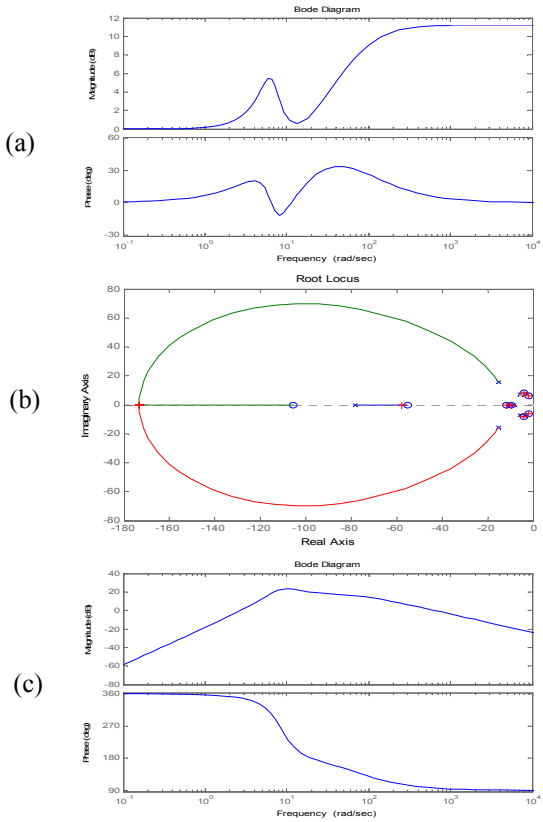

Fig. 4. (a) Bode plot for $K_{d11}(j\omega)$; (b) Roots' loci for K_{e11} design; (c) Bode plot for $K_{e21}(j\omega)$

3.2 The minimal control synthesis with error feedback (MCSEF) algorithm

The MCSEF algorithm is a derivative of the original MCS algorithm of (Stoten, 1989). MCS is an adaptive, model-referenced control strategy, which requires no *a priori* information on the plant dynamic parameters. Direct on-line computation of the adaptive, time-varying gains effectively enables the controller to accommodate parameter variations and uncertainties. Normally, the MCS algorithm comprises a parallel reference model, so that the state error between the model and the plant is ensured to be globally asymptotically stable. MCSEF was developed specifically for substructuring control, (Stoten and Hyde, 2006), in order to mirror the structure of the LSC algorithm; see Fig.5. Notwithstanding the fact that the parallel reference model has been removed, the numerical substructure can now be considered as an *ersatz* replacement for it.

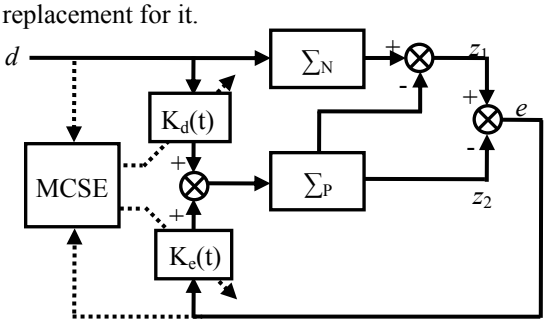

Fig. 5 MCSEF within a substructured environment

The hyperstability proof of the global asymptotic stability of MCSEF, within the given substructuring environment is based, is detailed in (Stoten and Hyde, 2006) and will not be repeated here. However, we do present the main controller equations in order to give some indication of the simplicity of the formulation. Thus, the control signal and adaptive gains are generated according to (18)-(20):

$$u(t) = K_d(t)\, d(t) + K_e(t)\, x_e(t) \tag{18}$$

$$K_d(t) = \alpha \int_0^t y_e(t)\, d(t)\, \mathrm{d}t + \beta y_e(t)\, d(t) \tag{19}$$

$$K_e(t) = \alpha \int_0^t y_e(t)\, x_e^{\mathrm{T}}(t)\, \mathrm{d}t + \beta y_e(t)\, x_e^{\mathrm{T}}(t) \tag{20}$$

where $\{\alpha, \beta\}$ are fixed scalar adaptive weights, which are selected empirically (*eg.* Stoten, 1992). The term x_e is the synchronisation state error and y_e is the output error, generated directly from x_e, in order to ensure strictly positive real dynamics for the hyperstability proof (Popov, 1973; Landau, 1979).

4. COMPARATIVE SIMULATION STUDIES

We now compare the relative performances of SiM1 under both LSC and LSC+MCSEF control.

4.1 Simulations with parameters set to nominal values

Swept sinusoidal excitations in the range 0.1-5.0Hz, duration 20s and amplitude 0.01m, are imposed on $\{\sum_{N1}, \sum_{N2}\}$ to simulate road perturbations. In addition, a 1.0s pure delay is imposed between the application of the disturbances on the front and rear wheels. Initially, the parameters of the

nonlinear dynamics of $\{\sum_{P3}\}$ are known perfectly, so that the LSC achieves excellent synchronisation between $\{\sum_{N1}, \sum_{N2}\}$ and $\{\sum_{P3}\}$; see Fig. 6, which also includes the emulated responses, labelled emu y_i. In particular, the synchronisation errors, $\{e_{y1}, e_{y2}\}$, are in the range of ±0.2mm. Fig. 7 shows the effect of additional MCSEF action, where the adaptive weights, $\{\alpha, \beta\}$, are set empirically to {1000, 100}. Only the front wheel/tyre responses are shown for the sake of brevity. Since the system parameters are well-known, the amount of adaptive action required is relatively small.

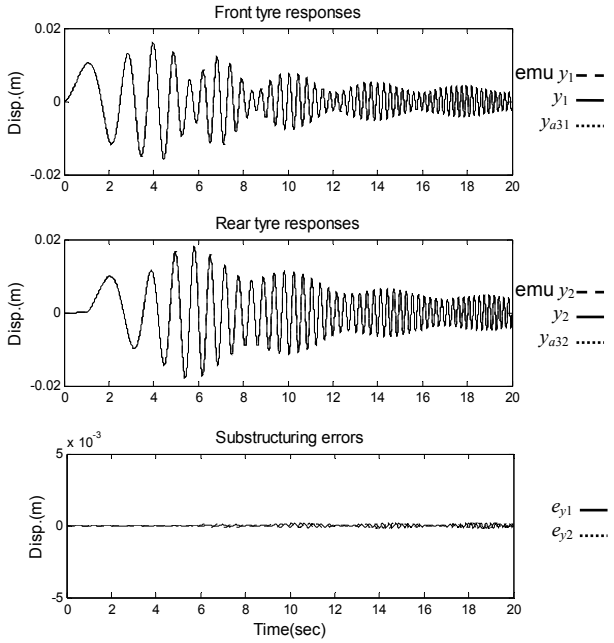

Fig. 6. LSC: nominal DSS parameter values

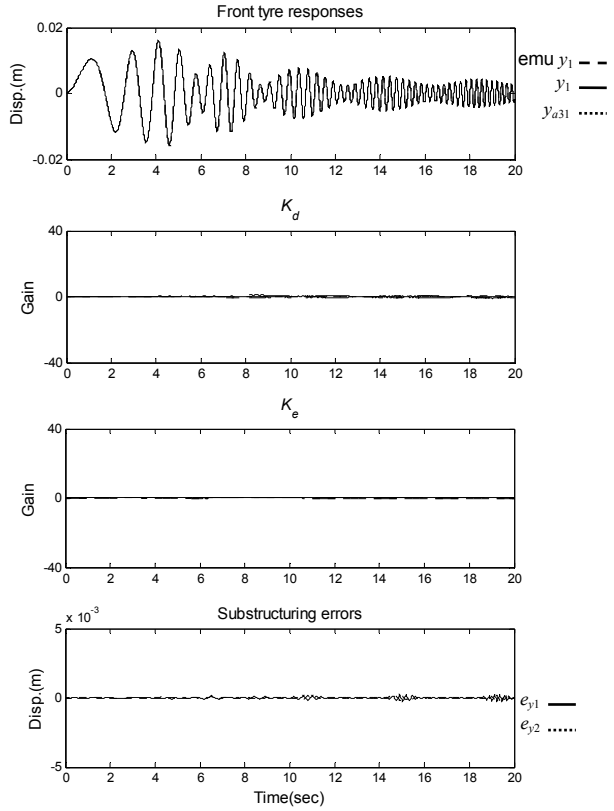

Fig. 7 MCSEF+LSC: nominal DSS parameter values

4.2 Simulations with parameter variations

In DSS implementations, the most significant cause for concern relates to unknown and changing actuator dynamics. Hence, we introduce a factor of 10 change in each of the actuator inner-loop parameters, $\{a_{31}, b_{31}\}$ and $\{a_{32}, b_{32}\}$, reducing them from 8.3 to 0.83. Fig. 8 shows the large substructuring errors, of the order ± 4mm, resulting from the use of LSC on its own. However, on introducing MCSEF, the resulting errors are now reduced by the adaptive effort, to values in the range ± 1mm; see Fig. 9.

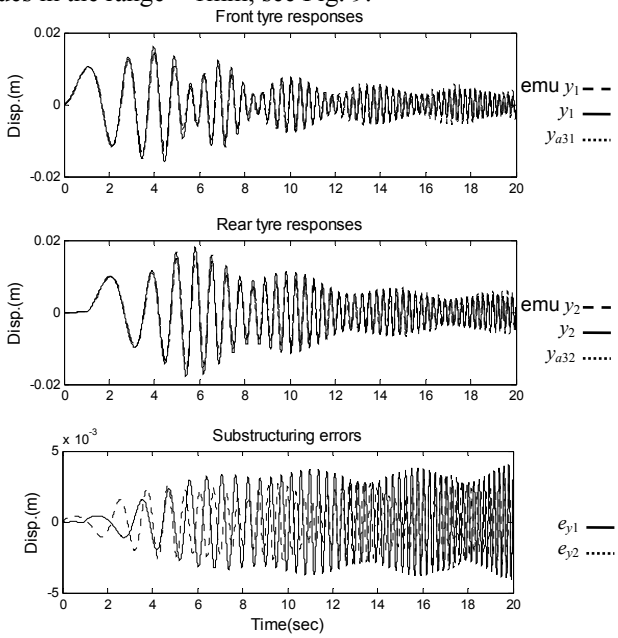

Fig. 8 LSC: DSS parameter values changed

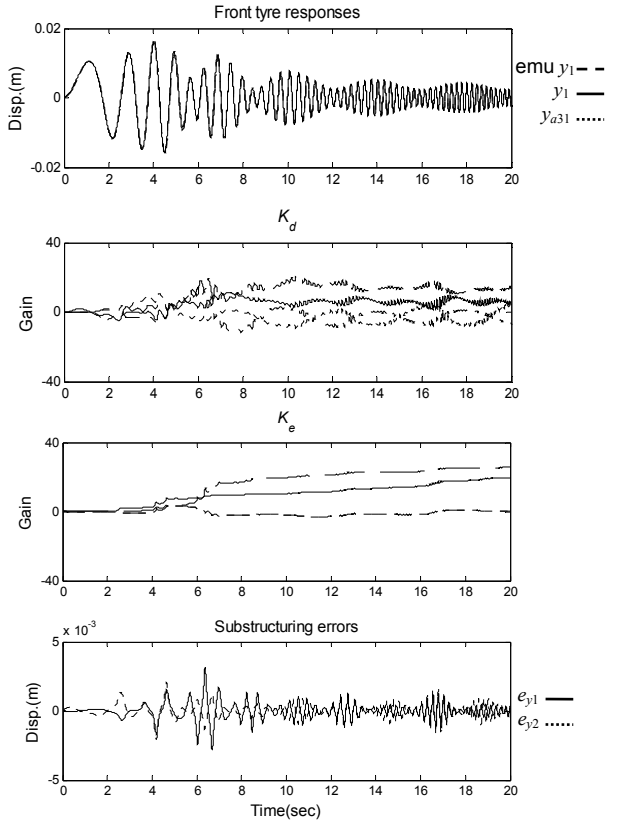

Fig. 9 MCSEF+LSC: DSS parameter values changed

5. CONCLUSIONS

The main conclusions to be drawn from this work are as follows:

- A generalised framework for dynamically substructured systems (DSS) has been established.
- We have shown that the DSS framework can be used to synthesise a linear substructuring controller (LSC), providing a basis for achieving the exacting levels of substructure synchronisation that are required. However, LSC performance degrades as parameter uncertainty increases.
- An extension of the adaptive minimal control synthesis (MCS) algorithm, which incorporates error feedback (EF), has been synthesised for the DSS problem. The new algorithm, MCSEF, can be viewed as an adaptive version of LSC.
- LSC and MCSEF can be used in parallel with one another for DSS control.
- Simulations showed that the addition of an MCSEF component enabled excellent synchronisation of DSS substructures, despite the presence of significant parameter uncertainties in the actuator dynamics.

Future work in this field will centre on the further development of the generalised dynamic framework of DSS and the corresponding synthesis and analysis of new LSC- and MCSEF-based controllers. In addition, as the construction of the quasi-motorcycle rig draws near to completion, experimental verification of the new DSS concepts will feature heavily in our future work.

Finally, the issue of whether to use displacement synchronisation (with force as an interaction constraint), or force synchronisation (with displacement as an interaction constraint), or a combination of these, has not yet been resolved. Preliminary results show that different modes of operation yield different levels of conditioning of the controllers, depending on the synchronisation variables that are used. Thus, another objective of our future research will be to solve this problem and thereby generate best-conditioned control strategies.

ACKNOWLEDGEMENT

The authors gratefully acknowledge the support of the UK Engineering and Physical Science Research Council, grant number EP/D036917 (*The adaptive control of generalised dynamically substructured systems*), in pursuance of this work.

REFERENCES

Blakeborough, A., Williams, M. S., Darby, A. P. and Williams, D. M. (2001). The development of real-time substructure testing, *Phil Trans R Soc Lond A*, 1869 – 1891.

Bonnet, P. A., Lim, C. N., Williams, M. S., Blakeborough, A., Neild, S. A., Stoten, D. P. and Taylor, C. A.(2007). Real-time hybrid experiments with Newmark integration, MCSmd outer-loop control and multi-tasking strategies, *Earthquake Engineering & Structural Dynamics*, **36**(1), 119 – 141.

Landau, Y. D. (1979). *Adaptive Control: The Model Reference Approach*, Marcel Dekker Inc., New York.

Popov, V. M. (1973). *Hyperstability of Control Systems*, Springer-Verlag, New York

Stoten, D. P. (1989). A minimal controller synthesis adaptive algorithm for environmental systems, *Science et Technique du Froid*, 277 – 286.

Stoten D. P. (1992). Implementation of MCS on a servohydraulic testing machine, *Proc I Mech E - Part I, Journ. Sys Cont Eng*, **206**, No I3, 189 – 194.

Stoten, D. P. and Benchoubane, H. (1990). Robustness of a minimal controller synthesis algorithm, *Int. J. Control*, **51**(4), 851-861.

Stoten, D. P. and Hyde, R. A.. (2006). Adaptive control of dynamically substructured systems: the single-input single-output case, *Proc. IMechE - Part I, Journ. Sys Cont Eng*, **220**, 63-79.

APPENDIX NOTATION FOR THE QUASI-MOTORCYCLE SUBSTRUCTURED SYSTEM

Table 2. Notations and Parameters

Parameter	Description	Values
Vehicle rigid body		
m_3	mass	160kg
J_3	moment of inertia	60kgm^2
L_3	length	2m
L_{31}, L_{32}	lengths from front and rear end to the centre of mass	0.8m, 1.2m
Front and rear suspension struts		
k_{31}, k_{32}	suspension spring stiffness	8000N/m
c_{31}, c_{32}	suspension damping	1120N/m s
Front and rear wheels/tyres		
m_1, m_2	overall mass	15kg
k_1, k_2	tyre radial stiffness	7000N/m
c_1, c_2	tyre radial damping	454N/m s
Nominal actuator parameters		
a_{31}, a_{32}	actuator denominator	8.3s^{-1}
b_{31}, b_{32}	actuator numerator	8.3m/V s